J Mater Sci (2011) 46:1058–1075
DOI 10.1007/s10853-010-4874-9

Influences of Si and Mg contents on microstructures of Al–*x*Si–*y*Mg functionally gradient composites reinforced with in situ primary Si and Mg_2Si particles by centrifugal casting

Xuedong Lin · Changming Liu · Yanbo Zhai · Kai Wang

Received: 30 January 2010 / Accepted: 26 August 2010 / Published online: 11 September 2010

Abstract Hypereutectic Al–*x*Si–*y*Mg functionally gradient composites reinforced with primary Si and Mg_2Si particles were fabricated by centrifugal casting. The influence of Si and Mg contents on microstructures of the Al–*x*Si–*y*Mg functionally gradient composites was investigated. Calculations of the volume fractions and the sizes of primary Si and Mg_2Si particles in the cross section of each tube along the radial direction from the inner-to-outer surface revealed that this type of gradient composite tube can be fabricated by centrifugal casting when the contents of Si and Mg are more than or equal to 19 and 4%, respectively. The tubes consist of an inner layer, the middle layer, and the outer layer measured in the radial direction on the cross section. The inner layer segregates blocky primary Si and Mg_2Si particles, the middle layer contains no primary Si and Mg_2Si particles, and the outer layer contains few primary Si and Mg_2Si particles. We compared resulting mean volume fractions and average sizes of produced primary Si and Mg_2Si particles with initial Si and Mg contents to determine their relationship in this process. The morphology of the Mg_2Si phase is another key factor in the formation of the composites. It was found that the blocky primary Mg_2Si particles have greater centroclinal velocity than that of primary Si particles due to the lower density of the Mg_2Si particles. The primary Si particles are pushed by blocky primary Mg_2Si particles. The two kinds of particles move toward the inner wall of the tube together during the solidification. A model of particles movement has been established according to the experimental results.

X. Lin (✉) · C. Liu · Y. Zhai · K. Wang
College of Material Science and Engineering, Chongqing University, Chongqing 400030, People's Republic of China
e-mail: dreamerdog@163.com

Introduction

Because of their excellent casting properties and wear resistance [1, 2], in recent years, Al–Si or Al–Mg_2Si alloys have been researched to fabricate industry parts, such as automotive aluminum cylinder liners, which are used as substitutes for iron cylinder liners. Using conventional fabrication techniques, the inner wall of the aluminum cylinder liner is covered with a hard-wearing layer incorporating reinforced particles, such as Si powders, applied by laser surface cladding or spray deposition methods [3–8]. However, these processes present several disadvantages such as inherent complexity process and high cost. Because of these disadvantages, the liners are hard to be extensively used in engineering. With the advent of functionally graded materials (FGM) [9, 10], several methods have been proposed to obtain the gradient structure in composite materials. The centrifugal method, proposed by Fukui et al., is one of the most effective methods for making these materials [11]. And several kinds of alloys, such as Al–Ni, Al–Mg–B, Al–Cu, and Al–Ni–Ti alloys, with the in situ reinforcement phase to obtain FGMs fabricated by centrifugal casting have been researched [12–18]. The reinforcement phase in the matrix can remarkably improve the mechanical properties of materials. The new method of centrifugal casting was adopted to produce FGM tubes using Al–Si alloy [19–21], with the goal of attaining the wear-resistant primary Si particles in the inner layer of tubes. The accumulation of Si particles in the inner layer of tubes, however, was not sufficient, due to the insignificant density difference between Si particles (2.33 g/cm^3) and Al melt (2.37 g/cm^3). The wear resistance of this kind of tube, therefore, cannot meet the requirements of a cylinder in an engine. Jian et al. fabricated hypereutectic Al–Mg_2Si alloy tubes and found that the volume

fraction of primary Mg_2Si particles in tubes can achieve 25–30 vol.% due to a greater density difference between Mg_2Si particles (1.88 g/cm^3) and Al melt (2.37 g/cm^3) [22, 23]. Compared with Si particles, however, the wear resistance of the material containing Mg_2Si particles is not optional, as the hardness of Mg_2Si particles is HV460, while that of Si particles is HV1000-1300. Qudong et al. fabricated Zn–27Al–*x*Mg–*y*Si alloy tubes by centrifugal casting [24, 25]. Using this method, the concentration of primary Si and Mg_2Si particles was enriched in the inner layer of the tubes. Changming et al. produced Al–19Si–5Mg alloy tubes by centrifugal casting and found that the primary Si and Mg_2Si particles were segregated and enriched in the inner layer of the tube. The accumulation of primary Si and Mg_2Si particles in the inner layer imparts a superior wear resistance to these tubes [26, 27].

Although composites reinforced by primary Si and Mg_2Si particles have been produced successfully with centrifugal casting using different alloys, the effect of Si and Mg contents on morphologies of primary Mg_2Si particles in alloys and the quantitative relations of Si and Mg contents to the volume fractions and sizes of primary Si and Mg_2Si particles have not been reported to date.

In this investigation, tubes of hypereutectic Al–*x*Si–*y*Mg alloy reinforced with in situ primary Si and Mg_2Si particles are fabricated. The quantitative relations of Si and Mg contents to the volume fractions and sizes of primary Si and Mg_2Si particles produced in the alloy were investigated, and the qualitative relation of Si and Mg contents to the morphology of primary Mg_2Si particles is discussed in this article. The purpose of this research is to optimize the Si and Mg contents of the hypereutectic Al–Si–Mg alloy and to optimize the incidence of reinforced particles in the inner layer of the tubes.

Experimental

Material compositions design

Seven compositions of hypereutectic Al–Si–Mg alloys were prepared by varying the contents of Si and Mg elements. These compositions were studied to determine the influences of different Si and Mg contents on microstructures of centrifugally cast aluminum matrix composites reinforced with primary Si and Mg_2Si particles. To study the effect on microstructures of the tube, one element is kept constant as the other is varied. The seven types of Al–Si–Mg alloys were divided into two groups. In the first group, three kinds of Al–Si–Mg alloys were prepared with different Mg levels, 2, 4, and 6%, with Si content kept constant at 20% (All data given are in weight percent (wt%) unless otherwise stated.) In the second group, four kinds of Al–Si–Mg alloys were prepared with different Si levels, 17, 19, 21, and 23%, with Mg content kept constant at 4%.

Material and sample preparations

Raw materials smelted to prepare the seven alloy compositions were commercial alloys of Al–18Si–1.2Mg and pure Si and Mg metals.

The raw materials were melted with an electronic-resistance furnace. After modification at 1,013 K, seven kinds of alloy melts were poured at temperature of 993 K into a hot mold of 473 K in a horizontal centrifugal machine. Tubes were formed under the centrifugal force which was characterized by G number of 128 (Fig. 1). Here, the G number is given by the following equation:

$$G = \omega^2 R/g, \tag{1}$$

where R is the radius of the cast tube (m) and ω is the mold rotation rate (in radians s^{-1}), and g is the acceleration due to gravity. The dimensions of the fabricated tubes are as follows: the outer radius is 51 mm, the length is 190 mm, and the thickness is 12 mm.

A tube was cut in the middle and one cross section was obtained. The cross section was polished and divided into six zones, which are a, b, c, d, e, and f, radically from the inner-to-outer surface (Fig. 2). Microstructures were observed with optical microscope (OM) and scanning electron microscope (SEM). Volume fractions and sizes of primary Si and Mg_2Si particles were measured at different regions in the cross section using Image PRO Plus software.

Results and analysis

Influence on microstructures of variant Mg levels at constant Si content

Three tubes were fabricated using Al–20Si–2Mg, Al–20Si–4Mg, and Al–20Si–6Mg alloys. Microstructures were micrographed at six regions at increasing radial distance of

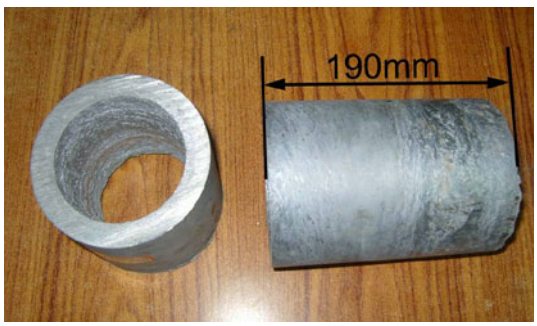

Fig. 1 Composite material tubes by centrifugal casting

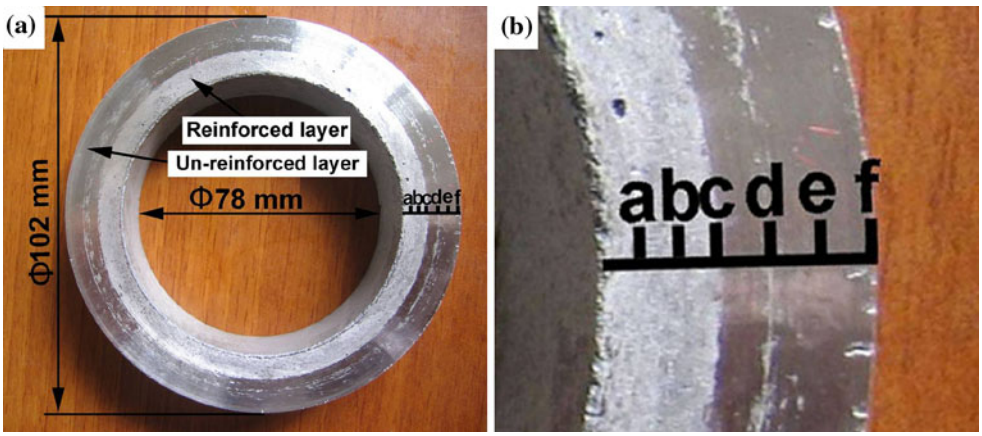

Fig. 2 Cross section of a tube. **a** Appearance of whole cross section and **b** six zone on the part of the cross section

the cross section and the distances of them from the inside of the tube were 1.5, 3.0, 4.5, 7.0, 9.5, and 12.0 mm. Their microstructures at six regions on the cross section are shown in Figs. 3, 5, and 7, respectively. The higher resolution images of microstructures of Al–20Si–2Mg and Al–20Si–4Mg alloys are shown in Figs. 4 and 6, respectively.

The phases marked in all images were analyzed by X-ray diffraction (XRD) and energy dispersive spectrometer (EDS) [27]. It is observed that microstructures of Al–20Si–2Mg tube produced by centrifugal casting were gray blocky primary Si particles with an average size of 50–70 μm, and net-shaped eutectic Mg_2Si and eutectic Si phases as shown in Fig. 4. The primary Si particles existed in all regions of the cross section of Al–20Si–2Mg tube as shown in Fig. 3. From the inner-to-outer surface, the incidence of blocky primary Si particles tended to gradually decrease.

Rather than the net-shaped eutectic phases in the Al–20Si–2Mg tube (Figs. 3, 4), black blocky Mg_2Si particles with an average diameter of 17–25 μm appeared in the cross section in the Al–20Si–4Mg tube as shown in Fig. 6b. Plenty of blocky Mg_2Si particles in the inner layer of the tube can be found as shown in Fig. 5a–c and even more Mg_2Si particles appeared in the Al–20Si–6Mg tube (Fig. 7), accompanied by primary Si particles. The formation of these blocky Mg_2Si particles facilitated the segregation of primary Si particles during the centrifugal process. Eventually, gradient composite tubes were produced with a substantial density of primary Si and Mg_2Si particles in the inner layer, no particles in the middle layer, and few particles in the outer layer.

Influence on microstructures of variant Si levels at constant Mg content

Microstructures at regions at increasing radial distance in the cross section of Al–17Si–4Mg, Al–19Si–4Mg, Al–21Si–4Mg, and Al–23Si–4Mg alloy tubes prepared by centrifugal casting are shown in Figs. 8, 10, 11, and 12, respectively. The distances at which microstructures were micrographed on the cross section along the radial direction from the inner-to-outer surface are 1.5, 3.0, 4.5, 7.0, 9.5, and 12.0 mm. Figure 9 shows the higher resolution image of microstructures of Al–17Si–4Mg alloy tube.

Comparing the microstructures shown in Figs. 10, 11, and 12, it can be seen that the microstructures of the inner layer of the Al–19Si–4Mg (Fig. 10), Al–21Si–4Mg (Fig. 11), and Al–23Si–4Mg (Fig. 12) alloy tubes contained many black blocky primary Mg_2Si particles with an average size of 17–25 μm and some gray blocky primary Si particles with an average size of 50–70 μm. The outer layer contained the eutectics of Al–Si and Al–Mg_2Si with few primary particles. Along the radial direction of the tubes, from the inner-to-outer surface, primary Si and Mg_2Si particles presented an obvious gradient distribution.

Distinct from the structures shown in Figs. 10, 11, and 12, the microstructures of Al–17Si–4Mg alloy tube, as shown in Figs. 8 and 9, showed some gray blocky primary Si particles and only the network eutectics of Al–Si and Al–Mg_2Si. There are no primary Mg_2Si particles in these images. It is deduced that 17% Si content is too low to form primary Mg_2Si particles as some of Si elements were consumed to form the primary Si particles. The content of Si was thus decreased to a point close to the eutectic content of Al–Si–Mg alloy. The primary Mg_2Si particles, therefore, could not be formed, no matter how high the Mg content. The higher content of Mg element caused plentiful network eutectic Mg_2Si to be formed in the matrix of the alloy. As more primary Si particles were found in the inner and outer regions than in the middle layer, the gradient distribution of the primary Si particles was not consistently formed.

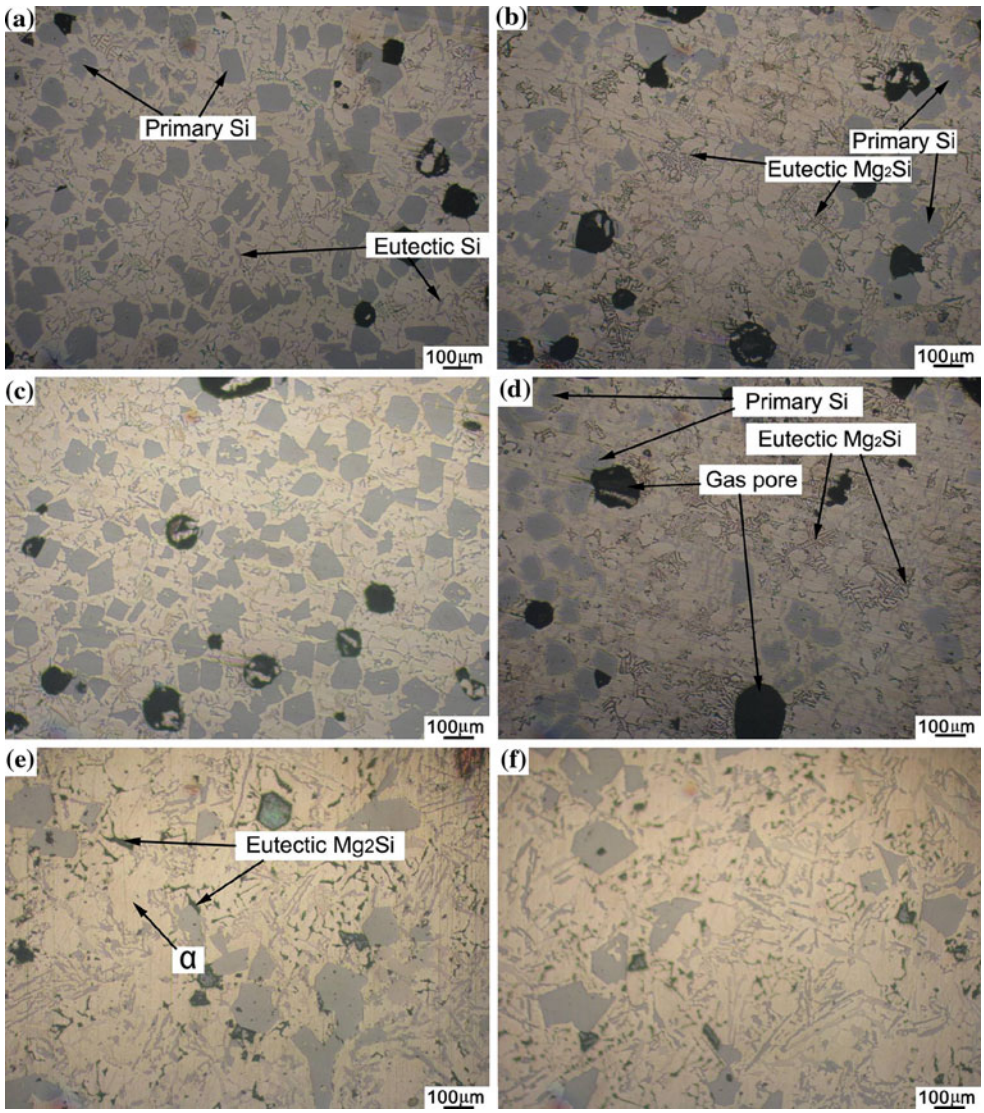

Fig. 3 Microstructures in different regions which are **a** 1.5 mm, **b** 3.0 mm, **c** 4.5 mm, **d** 7.0 mm, **e** 9.5 mm, and **f** 12.0 mm in the cross section of Al–20Si–2Mg tube

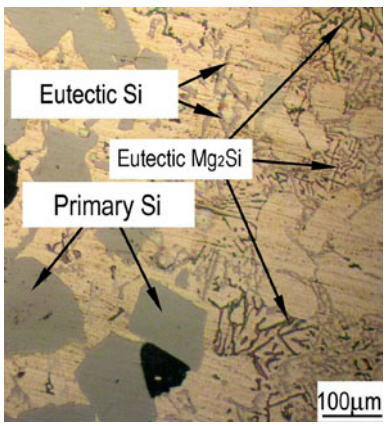

Fig. 4 Morphologies of Si and Mg_2Si of Al–20Si–2Mg tube

Particle volume fraction distributions of different Si and Mg contents

Relations of Mg content to volume fractions of primary Si and Mg_2Si particles along the radial direction of the tube

With the same 20% Si content, the volume fractions of primary Si and Mg_2Si particles of the three alloys with Mg contents of 2, 4, and 6% were measured (Figs. 13, 14).

From Figs. 13 and 14, it became evident that the primary Si particles had not segregated, but rather were scattered randomly throughout the tube with the Mg content of 2%. The volume fraction of primary Si particles was present in a range of 9.7–22.6 vol.%, with almost no formation of Mg_2Si particles. With the Mg content of 4%, the

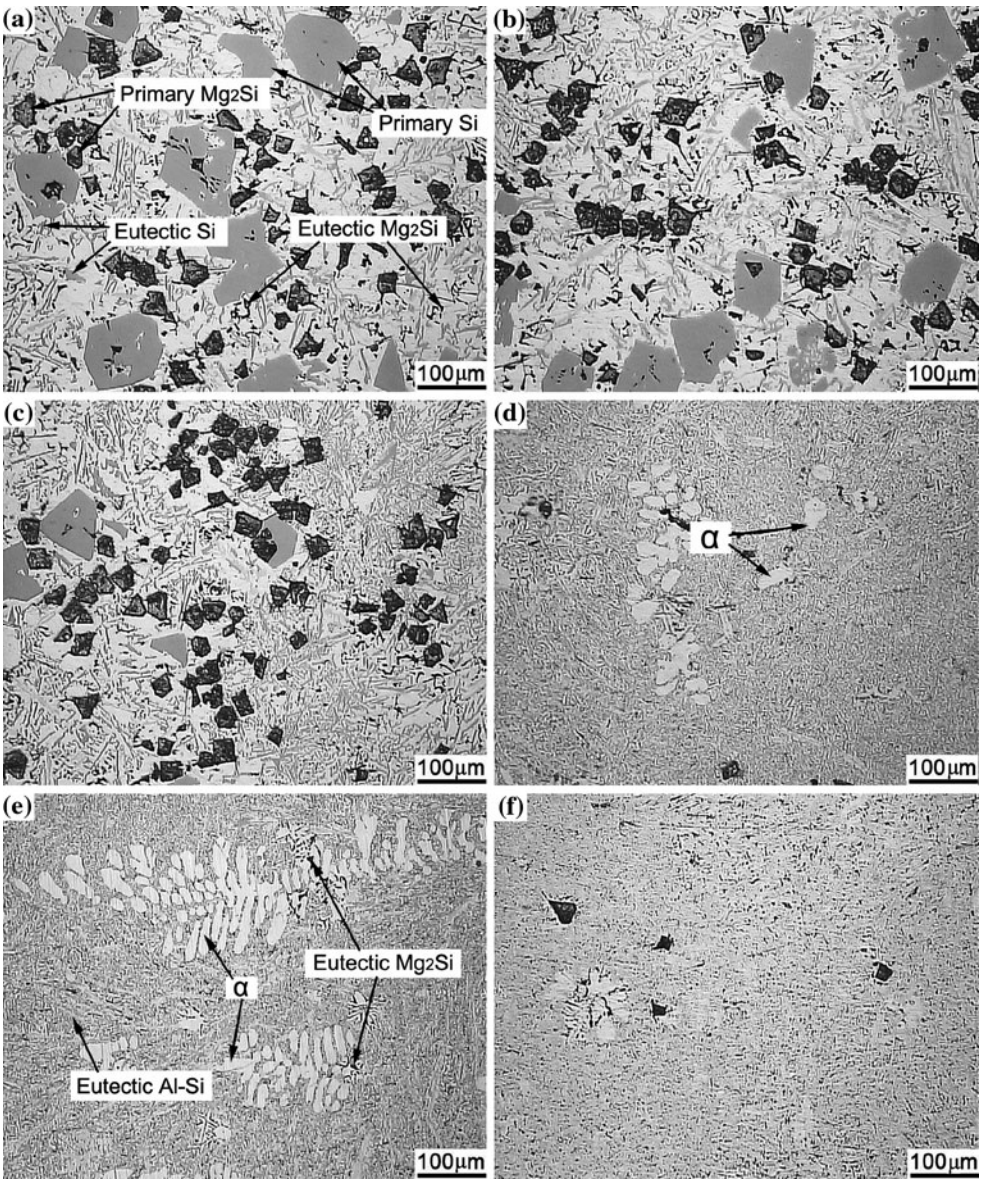

Fig. 5 Microstructures in different regions which are **a** 1.5 mm, **b** 3.0 mm, **c** 4.5 mm, **d** 7.0 mm, **e** 9.5 mm, and **f** 12.0 mm in the cross section of Al–20Si–4Mg tube

primary Si and Mg_2Si particles were segregated and enriched apparently in the inner region of 4.5 mm thickness. The highest volume fractions of the two kinds of particles were 15.6 vol.% as shown in Fig. 13 and 14.3 vol.% as shown in Fig. 14. With the Mg content of 6%, the primary Si and Mg_2Si particles were segregated and significantly enriched in the same region of the tube.

Relations of Si content to volume fractions of primary Si and Mg_2Si particles along the radial direction of the tube

With the content of Mg held constant at 4%, the volume fractions of primary Si and Mg_2Si particles in the four alloys with Si contents of 17, 19, 21, and 23% were measured (Figs. 15, 16).

It is observed from Fig. 15 that the primary Si particles were present in any position of the tube with a Si content of 17%. Many primary Si particles were found in the inner layer and outer layers, but few in the middle layer of the tube. No Mg_2Si particles were found in the tube (Fig. 16). For a Si content of 19%, the primary Si and Mg_2Si particles were obviously segregated and enriched in the inner layer of 4.5 mm thickness of the tube, with the majority of primary Si and Mg_2Si particles present in the inner wall of the tube. With the Si content of 21 and 23%, the primary Si and Mg_2Si particles were segregated and enriched remarkably in the inner region of the cross section.

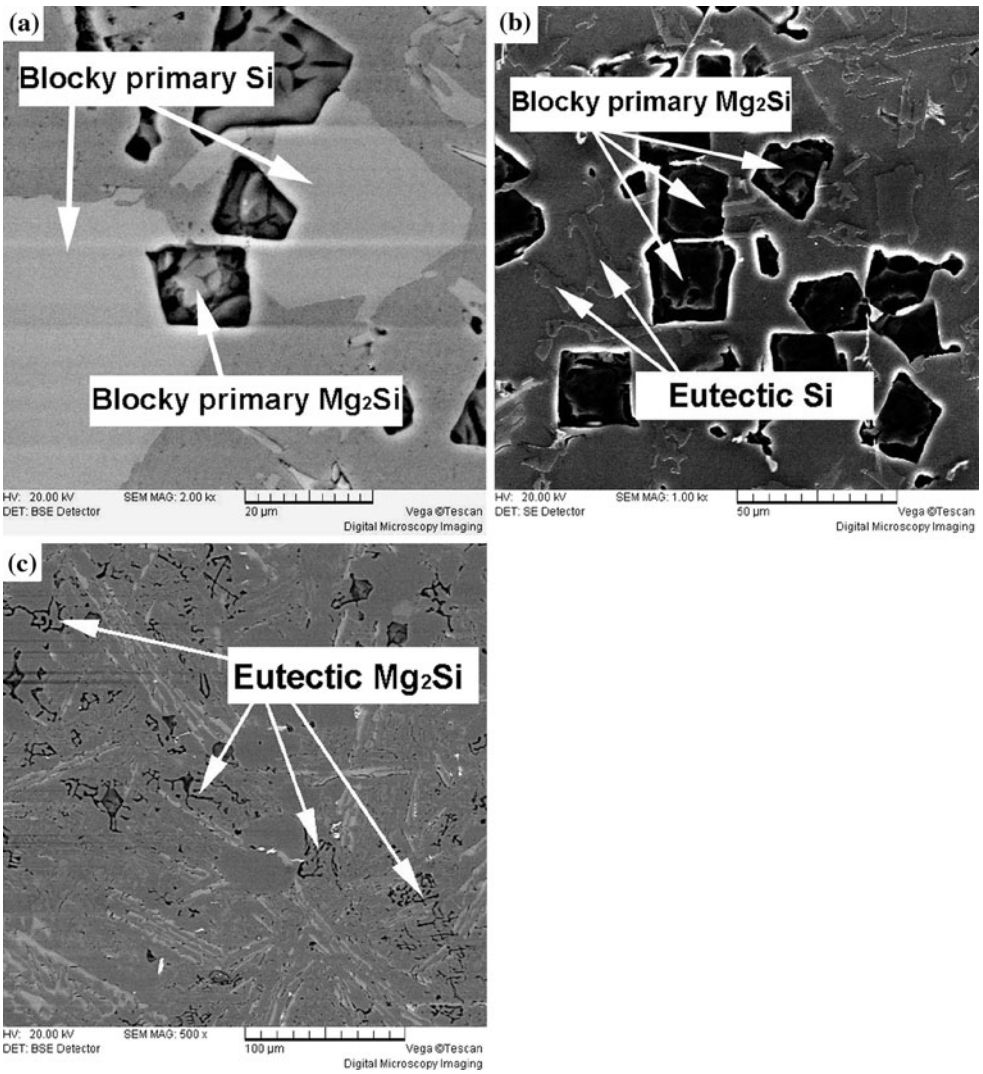

Fig. 6 Morphologies of Si and Mg_2Si of Al–20Si–4Mg tube: **a** blocky primary Si particles, **b** blocky primary Mg_2Si particles and net-shaped eutectic Si, and **c** net-shaped eutectic Mg_2Si

Relations of Si and Mg contents to the mean volume fractions of two kinds of particles in the inner layer of the tube

The mean volume fractions of primary Si and Mg_2Si particles in the region of 1.5–4.5 mm measured from inner-to-outer wall of the tubes were calculated, and the relations of contents of Si and Mg to the mean volume fractions of primary Si and primary Mg_2Si particles were obtained (Figs. 17, 18).

The mean volume fraction of Mg_2Si particles increased directly with Mg content, while the primary Si particles appeared to be formed in an inverse relationship with Mg content (Fig. 17). Specifically, with a constant 20% Si content, the mean volume fraction of primary Mg_2Si particles showed an ascending tendency, and primary Si particles, a marked decrease, as the Mg content increased from 2 to 6% (Fig. 17). With 2% Mg, no primary Mg_2Si particles were formed, while the average volume fraction of primary Si particles reached the greatest value of 20 vol.%. With 6% Mg, the average volume fraction of primary Si particles was at its lowest value of 5.2 vol.%, while that of primary Mg_2Si particles achieved its peak value of 19.2 vol.%. With 4% Mg, the mean volume fractions of the two particles reached values of 10.8 and 12.93 vol.%. As the content of Mg increased from 2 to 6%, the total aggregated volume fraction of the two kinds of particles showed an ascending trend from 20.0 to 24.4 vol.%.

With a constant 4% Mg content, it was found that the average volume fraction of primary Si particles in the inner layer first decreased, then increased, and that of

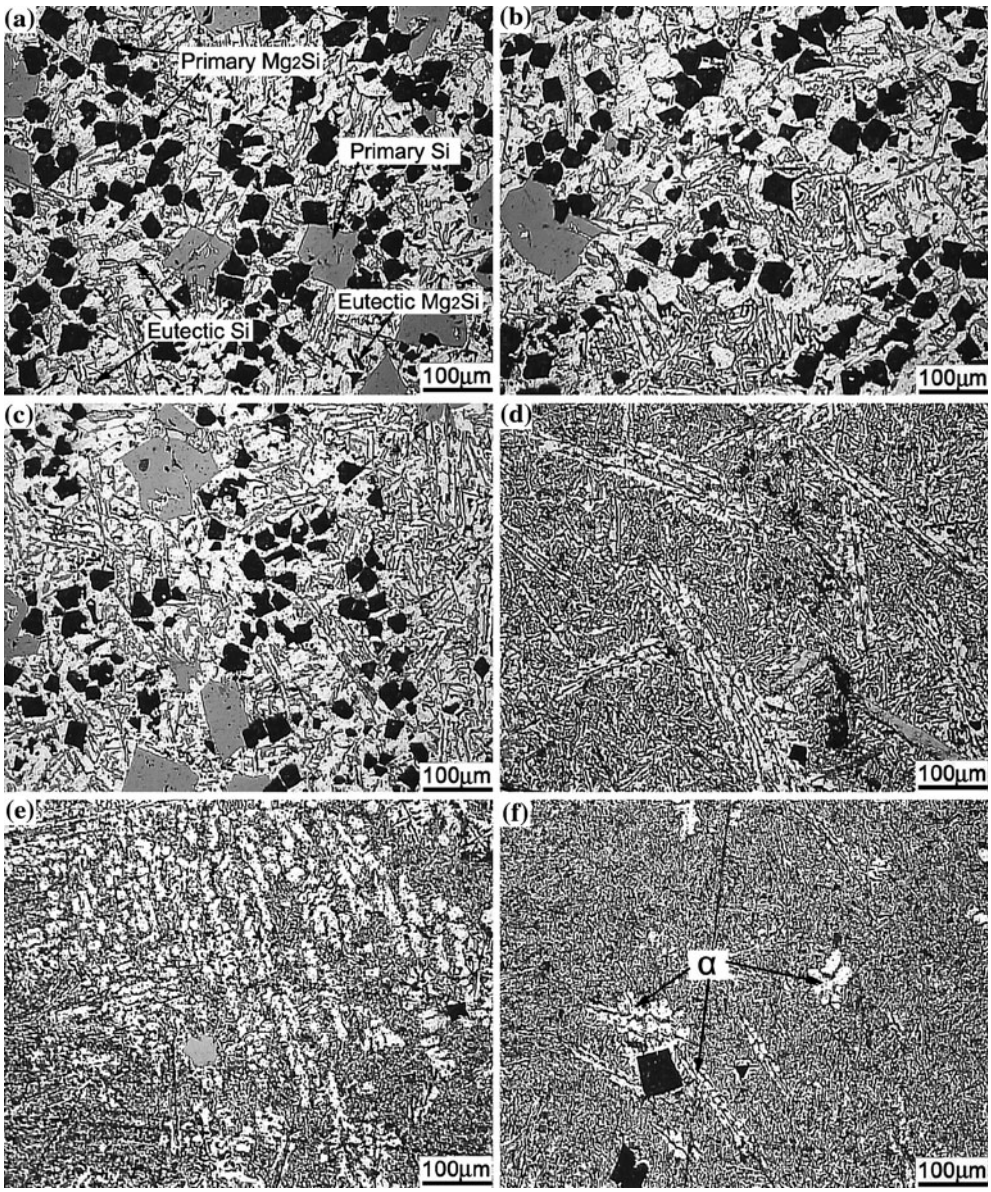

Fig. 7 Microstructures in different regions which are **a** 1.5 mm, **b** 3.0 mm, **c** 4.5 mm, **d** 7.0 mm, **e** 9.5 mm, and **f** 12.0 mm in the cross section of Al–20Si–6Mg tube

primary Mg_2Si particles rose at first and then generally remained steady as Si content increased (Fig. 18). With 17% Si, no primary Mg_2Si particles were formed. With 23% Si, the average volume fraction of primary Si particles reached the greatest value of 15.6 vol.%, while that of primary Mg_2Si particles was 12.2 vol.%. With 19% Si, the average volume fraction of the primary Si particles reached the lowest value of 7.5 vol.%, and that of primary Mg_2Si particles, reached the greatest value of 14 vol.%. As the content of Si increased from 17 to 23%, the total average volume fraction of the two kinds of particles presented an ascending tendency from 11.5 to 27.8 vol.% (Fig. 18).

Particle size distributions of different Si and Mg contents

Relations of Mg content to the sizes of two kinds of particles of the tube at constant Si content

With constant 20% Si, the primary Si and Mg_2Si particles sizes of three alloys with Mg contents of 2, 4, and 6% were measured. Values of particles sizes at different zones along the radial tube sections are shown in Figs. 19, 20.

Observing particle size distributions shown in Fig. 19, it can be seen that the primary Si particles of Al–20Si–2Mg in the inner and outer regions were larger than that in the

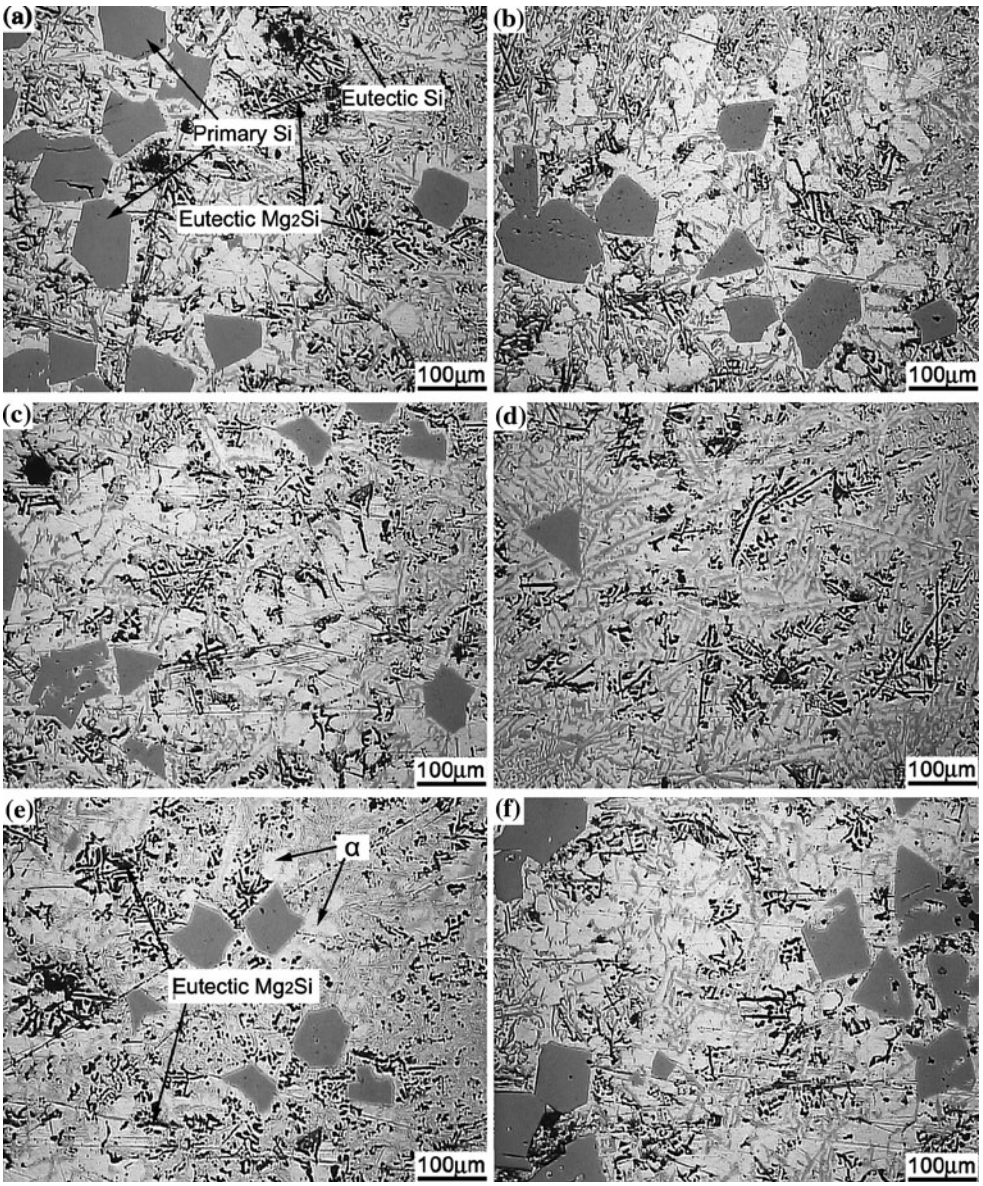

Fig. 8 Microstructures in different regions which are **a** 1.5 mm, **b** 3.0 mm, **c** 4.5 mm, **d** 7.0 mm, **e** 9.5 mm, and **f** 12.0 mm in the cross section of Al–17Si–4Mg tube

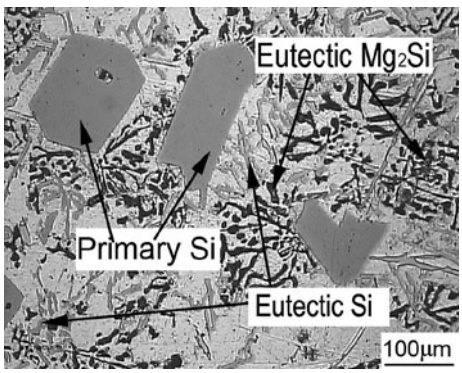

Fig. 9 Morphologies of Si and Mg_2Si of Al–17Si–4Mg tube

middle region of the tube. For the Al–20Si–4Mg and Al–20Si–6Mg alloys, however, the particles were segregated and enriched in the inner layer. Distribution rule of primary Si particle size in these two alloys was different from that of Al–20Si–2Mg alloy. This is related to the pushing effect of primary Mg_2Si particles to Si particles in the centrifugal force field. Under the pushing force, primary Si particles with different sizes were all segregated in the inner region.

As can be seen from Fig. 20, there were no primary Mg_2Si particles in the Al–20Si–2Mg alloy. The primary Mg_2Si particles of Al–20Si–6Mg were larger than that of Al–20Si–4Mg.

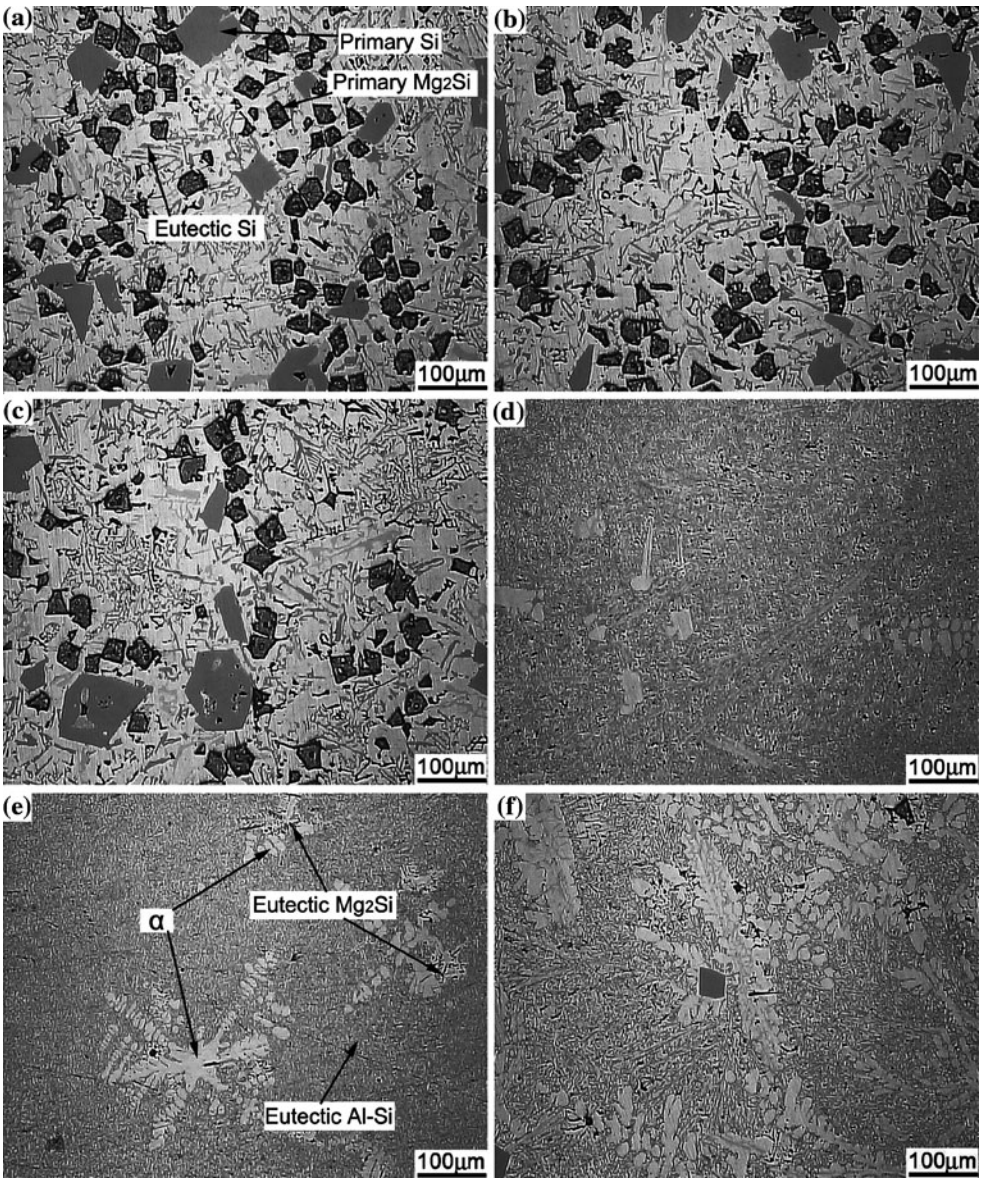

Fig. 10 Microstructures in different regions which are **a** 1.5 mm, **b** 3.0 mm, **c** 4.5 mm, **d** 7.0 mm, **e** 9.5 mm and **f** 12.0 mm in the cross section of Al–19Si–4Mg tube

Relations of Si content to the sizes of two kinds of particles of the tube at constant Mg content

With constant 4% Mg content, the primary Si and Mg_2Si particles sizes of four alloys with Si contents of 17, 19, 21, and 23% were measured (Figs. 21, 22).

From Fig. 21, it is seen that the size distribution of primary Si particles along the radial direction of Al–17Si–4Mg alloy had the same rule as that of Al–20Si–2Mg alloy shown in Fig. 19. For the Al–19Si–4Mg, Al–21Si–4Mg, and Al–23Si–4Mg alloys, the trend of primary Si particle size distribution in the inner layer was different from that of Al–17Si–4Mg alloy. Furthermore, it is seen that the primary Si particle size increased as the content of Si increased from 19 to 23%.

Variations of primary Si particle size in the inner layer are different from each other for Al–19Si–4Mg, Al–21Si–4Mg, and Al–23Si–4Mg alloys. For Al–19Si–4Mg alloy, the primary Si particle size in the inner layer of 1.5–4.5 mm showed an increasing tendency from 45.5 to 56.5 μm. The same rule occurred in the alloy of Al–23Si–4Mg alloy whose primary Si particle size in the same region varied from 63.1 to 68.8 μm. On the contrary, the variation of primary Si particle size in the inner layer of Al–21Si–4Mg alloy presented an inverse regulation whose size declined from 68.1 to 40.8 μm.

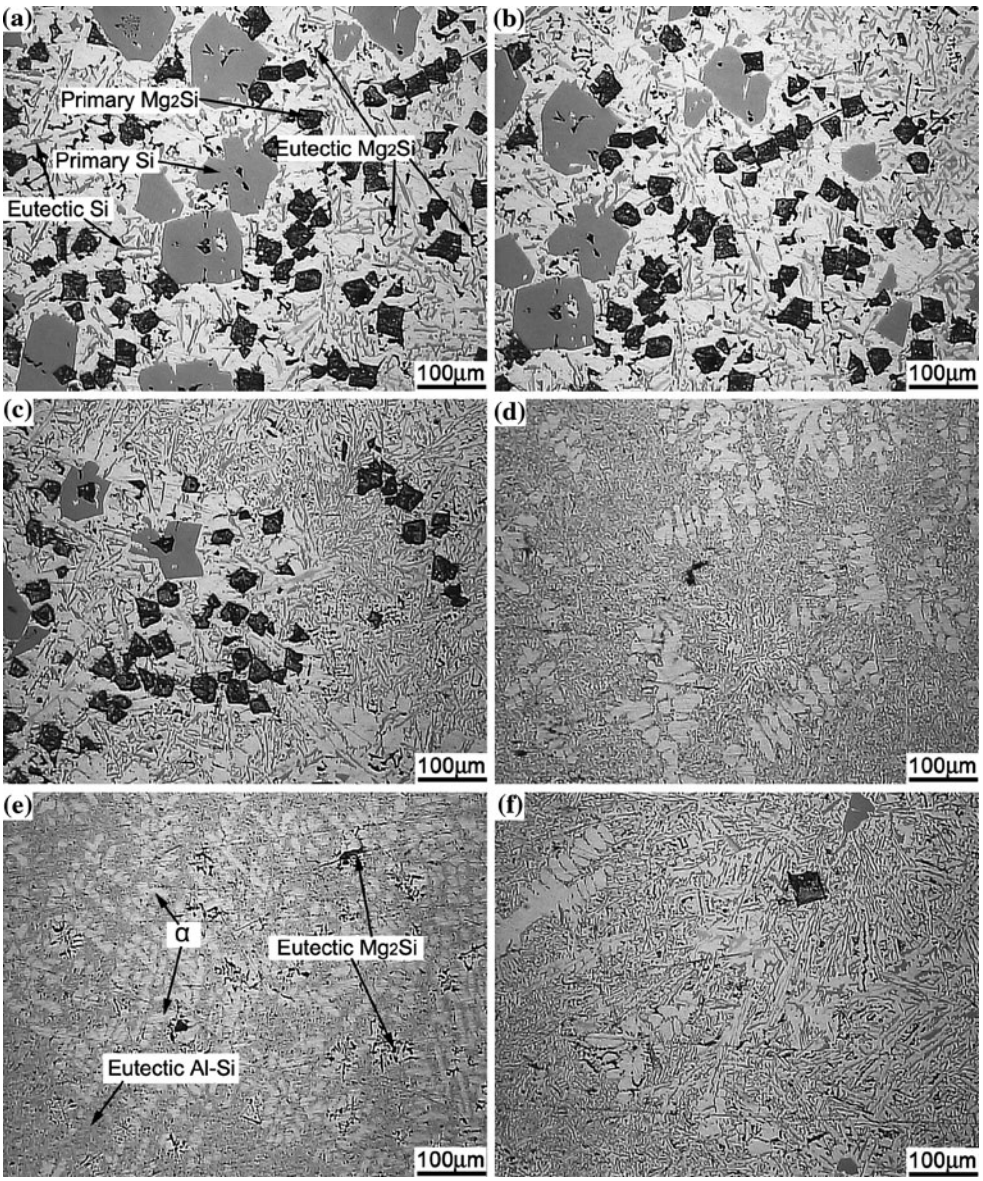

Fig. 11 Microstructures in different regions which are **a** 1.5 mm, **b** 3.0 mm, **c** 4.5 mm, **d** 7.0 mm, **e** 9.5 mm, and **f** 12.0 mm in the cross section of Al–21Si–4Mg tube

The size distributions of primary Mg_2Si particles of the four alloys are shown in Fig. 22. It can be seen that there were no primary Mg_2Si particles in the alloy of Al–17Si–4Mg. The differences of Mg_2Si particles sizes were very small among Al–19Si–4Mg, Al–21Si–4Mg, and Al–23Si–4Mg alloys.

Relations of Si and Mg contents to the average particles sizes in the inner layer of tubes

The average particles sizes of primary Si and Mg_2Si particles in the inner layer of tubes were calculated and the relations of Si and Mg contents to average particles sizes of alloys are shown in Figs. 23 and 24.

It was found from Fig. 23 that the average size of primary Mg_2Si particles presented a slight increase as the content of Mg varied from 4 to 6%, and the greatest average particle size was 23.2 μm. However, the average sizes of primary Si particles increased obviously from 52.9 to 63.8 μm with the Mg content increasing from 2 to 6%.

With same content of 4% Mg, as shown in Fig. 24, the average sizes of primary Mg_2Si particles of Al–19Si–4Mg, Al–21Si–4Mg, and Al–23Si–4Mg alloys were almost the same as the content of Si increased from 19 to 23% and they were 20.2, 19.9, and 19.8 μm, respectively. However, the average sizes of primary Si particles of the three alloys presented an increasingly trend and they were 50.2, 58.9, and 66.0 μm as content of Si varied from 19 to 23%.

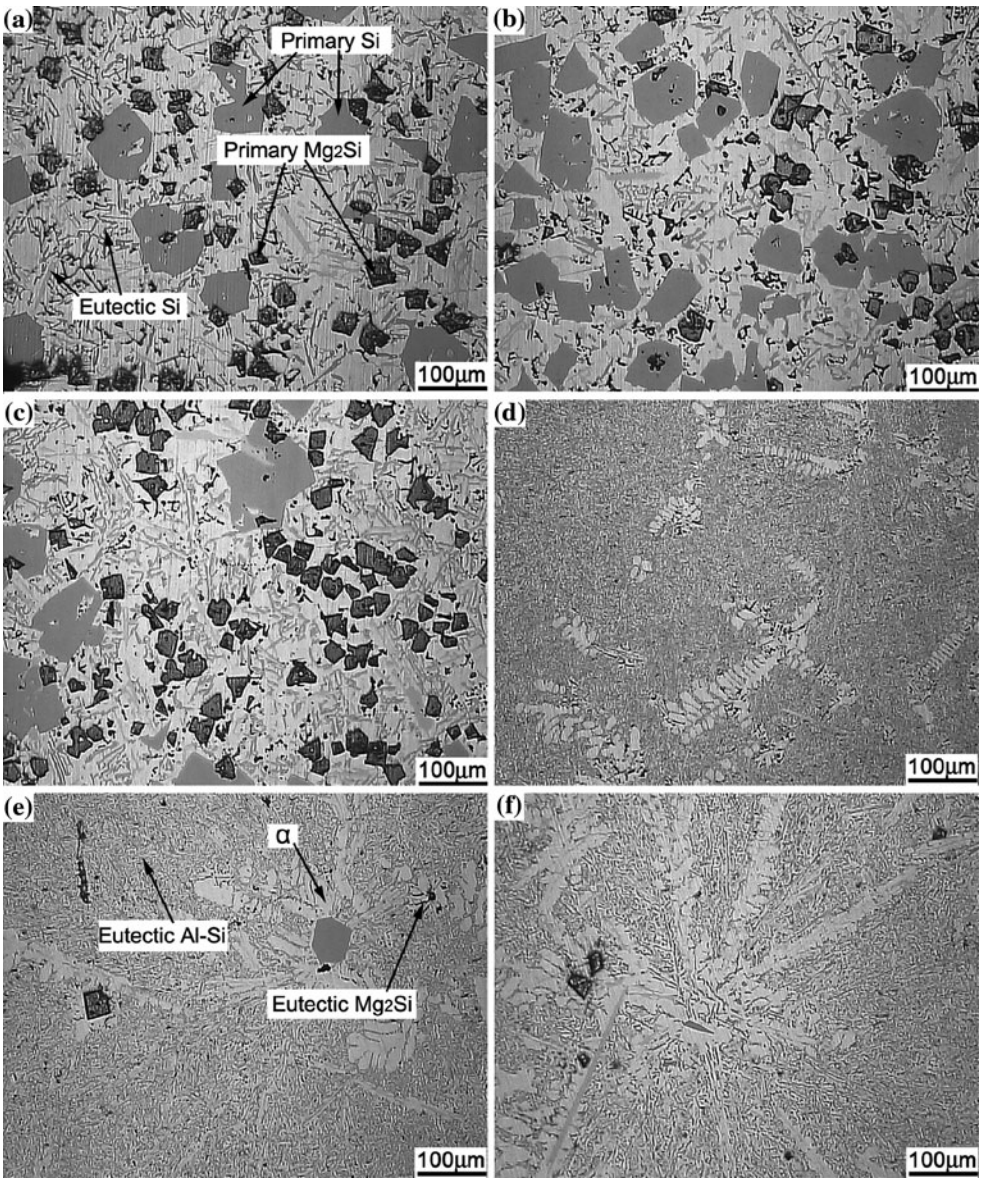

Fig. 12 Microstructures in different regions which are **a** 1.5 mm, **b** 3.0 mm, **c** 4.5 mm, **d** 7.0 mm, **e** 9.5 mm, and **f** 12.0 mm in the cross section of Al–23Si–4Mg tube

Discussions

Model establishment of primary particles movement

From the microstructures of tubes fabricated with seven different compositions of alloys, it is seen that alloys of Al–20Si–2Mg and Al–17Si–4Mg cannot form the gradient composites. The main reason for this is the missing of primary Mg_2Si particles in these alloys. With the occurrence of blocky primary Mg_2Si particles in other five alloys which had higher contents of Si and Mg, the model of particles migrating and enriched in the inner layer of tubes has been established as shown in Fig. 25.

Taking the Al–19Si–4Mg alloy, for example, the process of particles movement in the melt along the thickness direction of the tube was divided into four stages.

In the first stage, a few primary Si particles precipitate from the melt and are fixed in the outer region of the tube because of the chilling effect of the mold as shown in Fig. 25a.

In the second stage, plenty of primary Si particles show up and are pushed into the inner layer under the centrifugal force as shown in Fig. 25b.

The third stage should be made clear. With the temperature going down, the primary Mg_2Si particles start to form in the melt, and simultaneously, a few primary Si

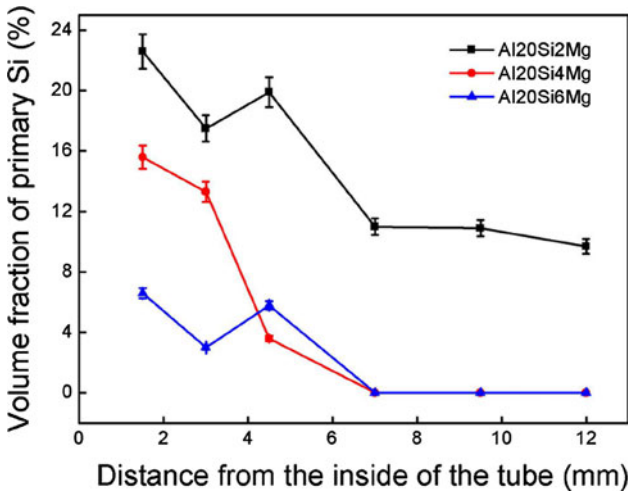

Fig. 13 Relation of Mg content to volume fractions of primary Si particles along the radial direction of the tube at constant 20% Si content

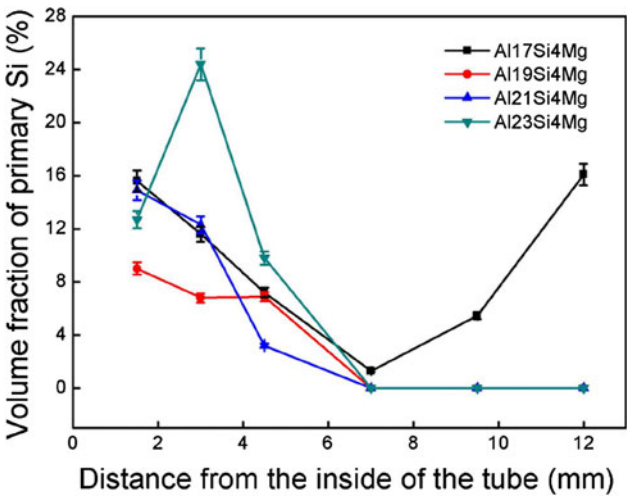

Fig. 15 Relation of Si content to volume fractions of primary Si particles along the radial direction of the tube at constant Mg of 4%

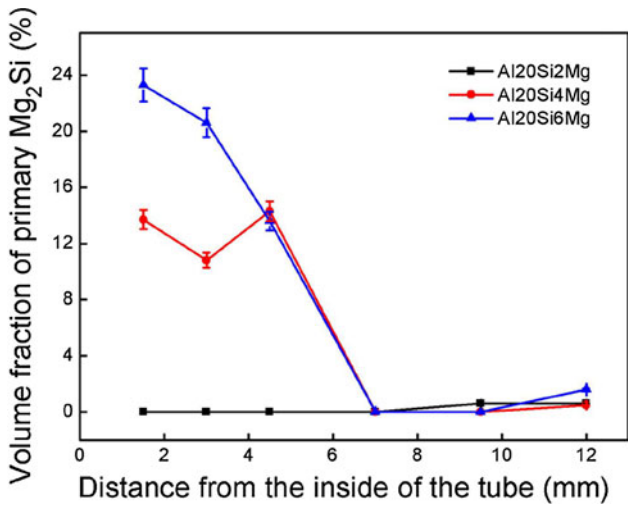

Fig. 14 Relation of Mg content to volume fractions of primary Mg_2Si particles along the radial direction of the tube at constant Si of 20%

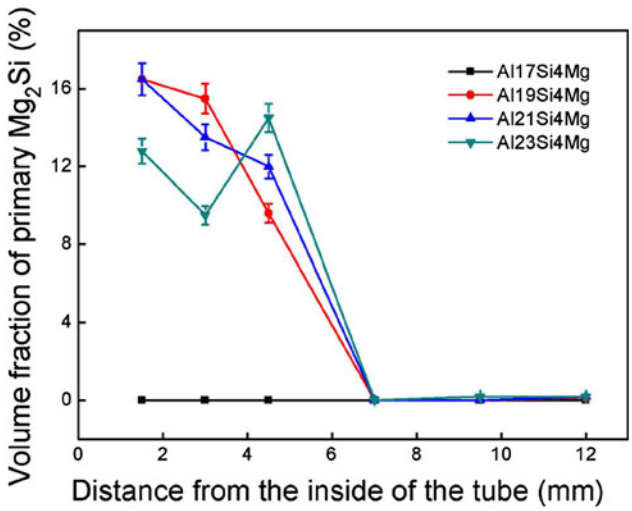

Fig. 16 Relation of Si content to volume fractions of primary Mg_2Si particles along the radial direction of the tube at constant Mg of 4%

particles generate continuously. Because of viscosity increasing due to the temperature decreasing and the particles generating continuously from the melt [28], and, a very small density difference between Si particles and Al melt, it is difficulty for Si particles themselves to migrate in this stage. The movement velocities of primary Si and Mg_2Si particles, υ, are described as follows according to Stocks equation:

$$\upsilon = \frac{2(\rho_{Al} - \rho_p)R_p^2\omega^2 r}{9\eta}, \tag{2}$$

where ρ_p is the density of solid particles, ρ_{Al} is the density of aluminum melt, ω is the rotating rate, r is the distance from location of solid particles to rotating center, η is the viscosity of melt, and R_p is the radius of solid particles.

According to Eq 2, the ratio of velocities of primary Si and Mg_2Si particles is obtained with Eq 3 as shown as follows. It is known from Eq 3 that velocity of Mg_2Si particles is over two times greater than that of Si particles. Hence, the primary Mg_2Si particles will push the primary Si particles to move toward the inner wall of the tube as shown in Fig. 25c.

$$\frac{\upsilon_{Mg_2Si}}{\upsilon_{Si}} = \frac{\left(\rho_{Al} - \rho_{Mg_2Si}\right)R_{Mg_2Si}^2}{(\rho_{Al} - \rho_{Si})R_{Si}^2} \approx 2.1, \tag{3}$$

where $R_{Mg_2Si} = 12.5\ \mu m$, $R_{Si} = 30\ \mu m$, $\rho_{Al} = 2.37\ g/cm^3$, $\rho_{Si} = 2.33\ g/cm^3$, and $\rho_{Mg_2Si} = 1.88\ g/cm^3$.

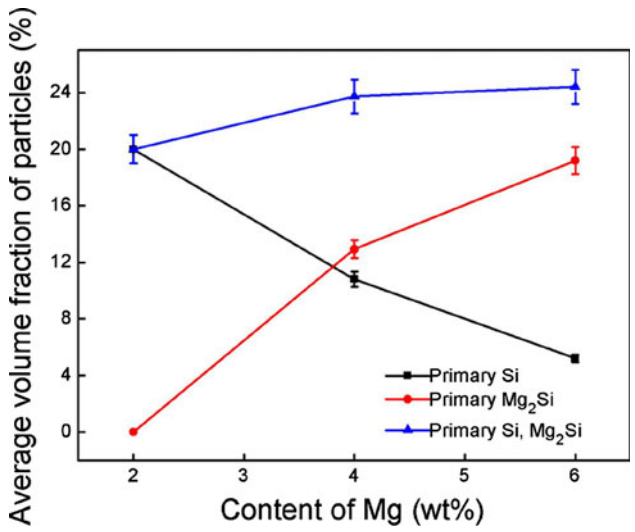

Fig. 17 Relation of Mg content to the average particle volume fractions of primary Si and primary Mg_2Si in the inner layer at constant Si of 20%

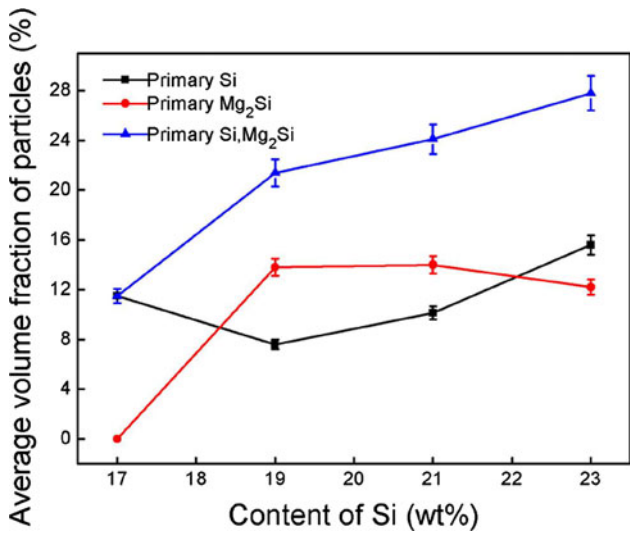

Fig. 18 Relation of Si content to the average particle volume fractions of primary Si and primary Mg_2Si in the inner layer at constant Mg of 4%

At last stage, the two kinds of primary particles are rich in the inner layer and the gradient composites tubes has been fabricated as shown in Fig. 25d. Eutectics Si and Mg_2Si exist in the middle layer. A few small primary Si particles stay in the outer layer of the tube because of the chilling effect of steel mold.

For the Al–17Si–4Mg and Al–20Si–2Mg alloys, because of no occurrence of primary Mg_2Si particles in the second stage during solidification, the primary Si particles could not migrate or be pushed to the inner layer of tubes as shown in Fig. 26b. Hence, the primary Si particles distribute in all regions of the cross section and the gradient

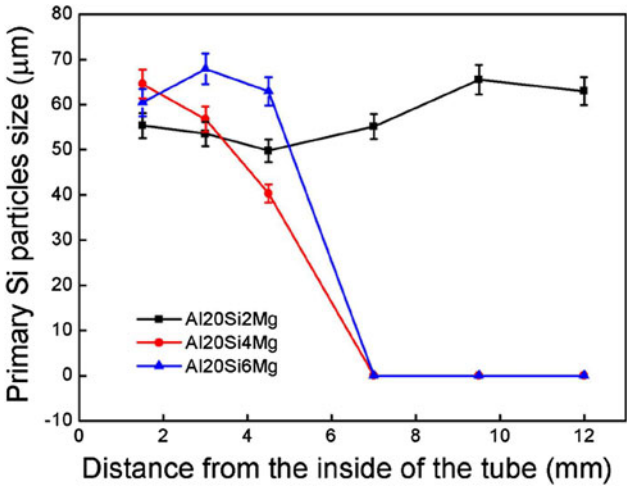

Fig. 19 Relation of Mg content to particles sizes of primary Si along the radial direction of the tube at constant Si of 20%

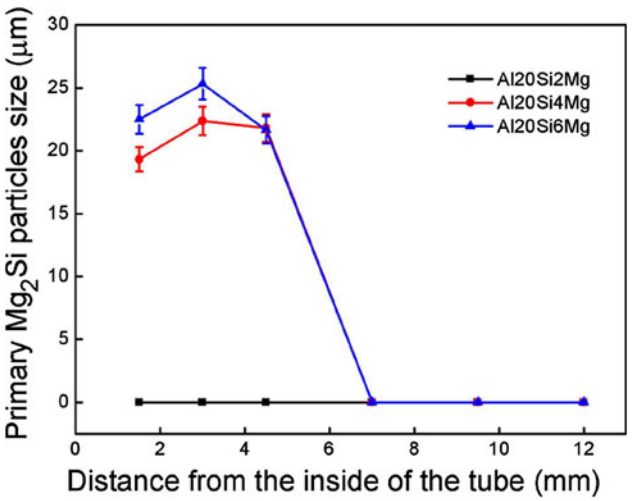

Fig. 20 Relation of Mg content to particles sizes of primary Mg_2Si along the radial direction of the tube at constant Si of 20%

functionally composites cannot be acquired as shown in Fig. 26c.

Determination of Si and Mg contents

Comparing the microstructures of the seven alloy tubes mentioned above, it was found that reinforced Mg_2Si particles were not always present in the inner layer of the tube in Al–*x*Si–*y*Mg alloys fabricated by centrifugal casting despite the presence of dense primary Si particles, such as Al–17Si–4Mg alloy. It was observed in Figs. 4 and 9 that Mg_2Si phase presented network or worm-like morphology of eutectic structures and there were no blocky primary Mg_2Si particles in the matrix, and, the gradient distribution of primary Si particles cannot be obtained. Except Al–17Si–4Mg and Al–20Si–2Mg alloys, the other five

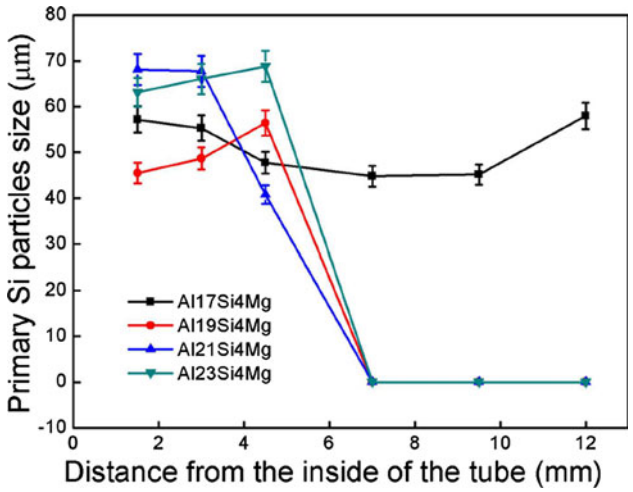

Fig. 21 Relation of Si content to particles sizes of primary Si along the radial direction of the tube at constant Mg of 4%

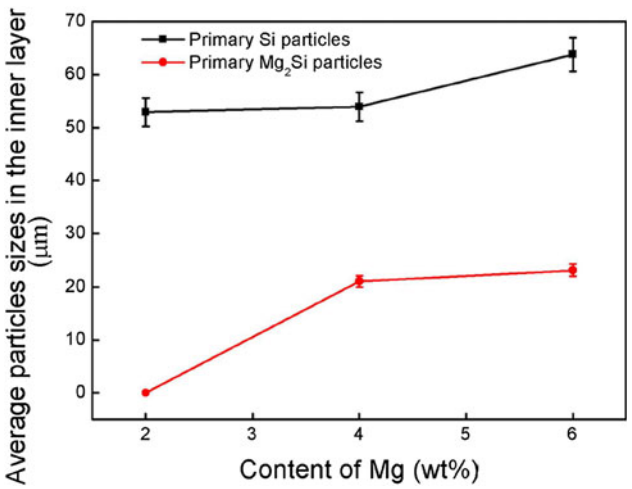

Fig. 23 Relation of Mg content to the average particles sizes of primary Si and Mg_2Si in the inner layer at constant Si of 20%

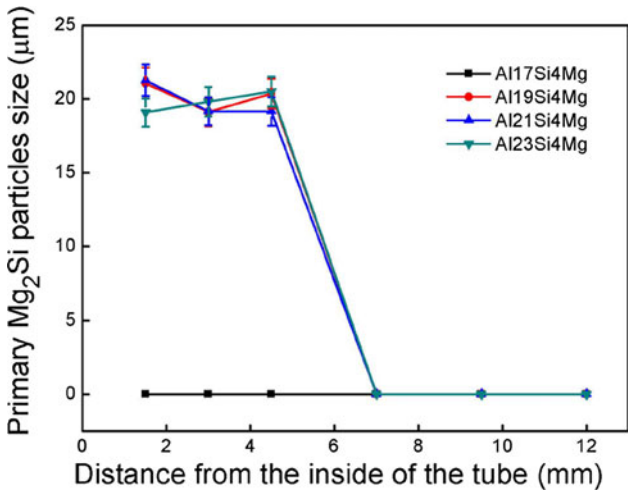

Fig. 22 Relation of Si content to particles sizes of primary Mg_2Si along the radial direction of the tube at constant Mg of 4%

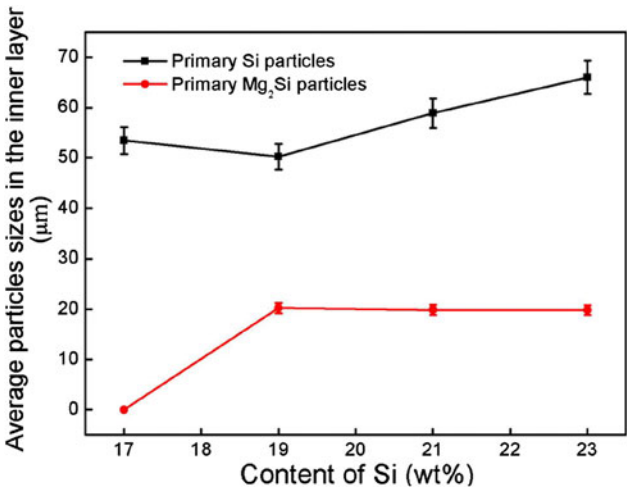

Fig. 24 Relation of Si content to the average particles sizes of primary Si and Mg_2Si in the inner layer at constant Mg of 4%

alloys showed both existing primary particles of Mg_2Si and Si, such as Al–19Si–4Mg as shown in Fig. 10. The Al–Si–Mg gradient composites were produced by centrifugal casting. Although the Mg_2Si phase existed in all seven alloys, the Al–Si–Mg gradient composites were obtained by centrifugal casting only when the Mg_2Si phase appeared with the feature of primary blocky particles, rather than the feature of network or worm-like eutectic structures. The existence of the blocky primary Mg_2Si particles contributed to the improvement of reinforcement of the alloy and to the improvement of the movement speed of primary Si particles toward to the inner layer of the tube as well. The contents of Si and Mg in the alloy, therefore, should be over or equal to 19% for Si element and over or equal to 4% for Mg element to obtain both primary Si and Mg_2Si particles.

Forming process of varied morphologies of Mg_2Si

Comparing the microstructure of Al–20Si–2Mg alloy with that of Al–20Si–4Mg alloy, it was found that the gray blocky primary Si particles appeared in both alloys, but the black blocky primary Mg_2Si particles presented only in the tube with the Mg content of 4%. From the microstructures of Al–17Si–4Mg and Al–19Si–4Mg alloys, it is observed that the blocky primary Si particles were showed in both alloys, but the blocky primary Mg_2Si particles were formed only in the tube with the Si content of 19%. As a result, the formation of the blocky primary Si and Mg_2Si particles depended on both contents of Si and Mg.

Combined with the Al–Si–Mg alloy equilibrium solidification diagram, for the Al–20Si–2Mg alloy, the primary Si particles precipitate during the initial solidification

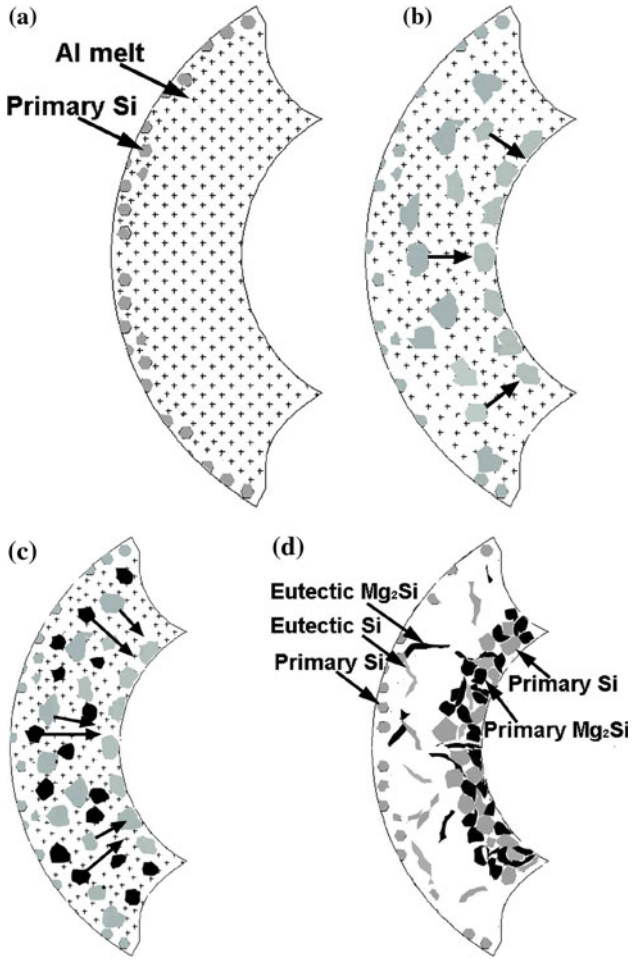

Fig. 25 The model of pushing effect of primary Mg_2Si particles to primary Si particles

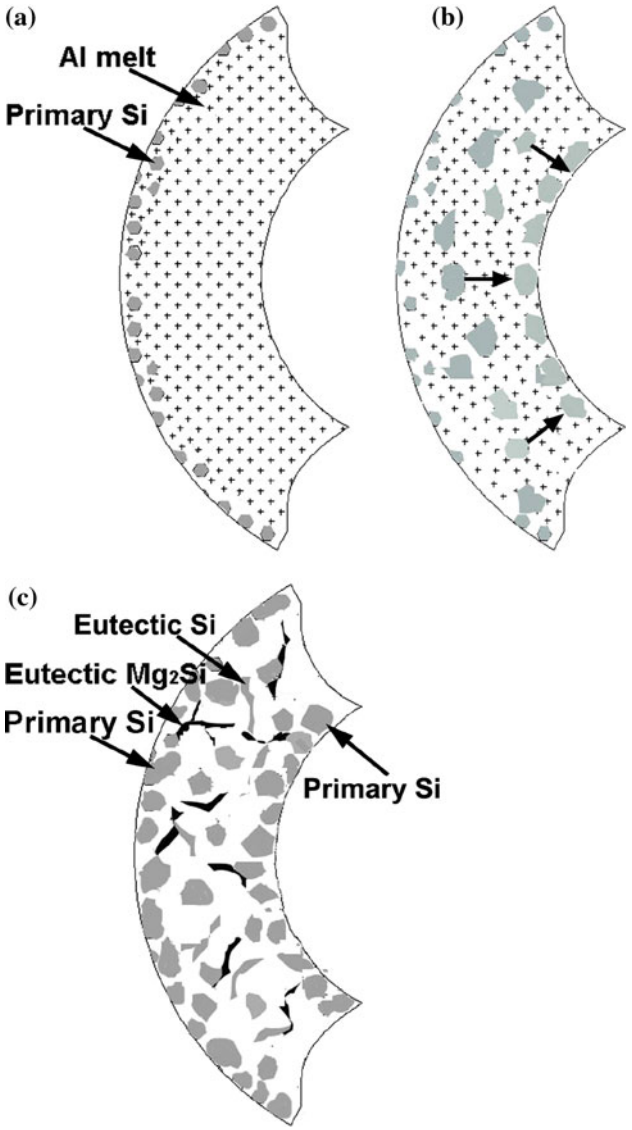

Fig. 26 The model of no pushing effect of primary Mg_2Si particles to primary Si particles

stage, and the reaction: L → L + Si takes place. With the temperature of the melt falling off, the number of primary Si particles increased, and the content of Si in the melt was continuously reduced. The content of 2% Mg in the melt was too small to form primary Mg_2Si particles when the melt dropped to the temperature of forming the particles. After the temperature of the melt and the Si content in the melt reduced further, the eutectic reactions: L → Al + Si, L → Al + Mg_2Si, and L → Al + Si + Mg_2Si take place and the dendritic or network or worm-like eutectic structures of Al–Si, Al–Mg_2Si, and Al–Si–Mg_2Si formed in the rest of the melt until the completion of solidification.

For Al–17Si–4Mg alloy, the content of Si decreased continually as the primary Si particles formed with the dropping temperature of the melt. The Si atoms in the melt were consumed to the extent that primary Mg_2Si particles cannot be formed in spite of a higher Mg content when temperature of the melt declined to the temperature of forming the Mg_2Si particles. The abundant Mg atoms only formed eutectic Mg_2Si of network or worm-like structures with the rest Si atoms in the melt in the subsequent eutectic reaction. As for the alloys of Al–19Si–4Mg (Fig. 10), Al–21Si–4Mg (Fig. 11), and Al–23Si–4Mg (Fig. 12), although many Si atoms were consumed during the formation of primary Si particles, a sufficient number of Si atoms remained in the melt to form primary Mg_2Si particles with the Mg atoms.

Briefly, only both Si and Mg atoms reached critical values at which the primary Si and Mg_2Si particles can be formed in the melt. Otherwise, the Mg_2Si was formed in the form of eutectic structure in the last period during solidification.

Determination of particle average volume fraction

As shown in Fig. 17, when Si content was 20%, primary Mg_2Si particles formed when the Mg content ≥4%.

When the Mg content reached 6%, more primary Mg_2Si particles formed in the Al–20Si–6Mg alloy. When the primary Si particles began to precipitate from the melt, Si atoms were consumed continuously. However, for 20% Si, there were still an abundance of Si atoms left in the melt. During that process, the remaining Si atoms met plentiful Mg atoms, forming more primary Mg_2Si particles. With the Mg content of 6%, more Mg_2Si particles appeared. Meanwhile, because the formation of more primary Mg_2Si particles consumed more Si atoms, the average volume fraction of primary Si particles of Al–20Si–6Mg alloy was less than that of Al–20Si–4Mg alloy. The amount of primary Si particles in Al–20Si–2Mg alloy was the greatest among the three alloys because no primary Mg_2Si formed in that alloy, leaving free enough Si atoms to form the Si particles.

The same process occurred in the Al–17Si–4Mg alloy (Fig. 18). No primary Mg_2Si particles formed and no Si atoms were consumed; therefore, many primary Si particles were obtained in the alloy. With a constant content of 4% Mg, the average volume fraction of primary Si particles showed an ascending tendency with Si content from 19 to 23%. Comparing the alloy with 19% Si, the alloy with 23% Si had more Si atoms, so when the primary Si particles began to precipitate from the melt, the Al–23Si–4Mg alloy had more Si atoms to form more primary Si particles. During the formation of primary Si, some Si atoms were consumed and the other Si atoms formed primary Mg_2Si with the Mg atoms. As the Mg content stayed constant at 4%, the average volume fraction of primary Mg_2Si particles was similar in alloys with Si content from 19 to 23%.

The relationship between the average volume fractions of primary Si and Mg_2Si particles and the contents of Si and Mg was studied as well. The first group of experimental materials included three kinds of Al–Si–Mg alloys: Al–20Si–2Mg, Al–20Si–4Mg, and Al–20Si–6Mg. During solidification, the primary Si particles precipitated in the first phase. In the second phase, the primary Mg_2Si started to appear from the melt, with the primary Si continuously forming in the melt. In the third phase, the eutectic structures of Al–Si, Al–Mg_2Si, and Al–Si–Mg_2Si formed. Thus, the Si atoms were consumed in reactions of all the three phases. For the Al–Si alloy, eutectic reaction of the melts takes place when the Si content reached 12.6%. For Al–20Si–yMg, it was assumed that the remaining 7.3% content of Si atoms were consumed to form primary Si and Mg_2Si particles. From the equation of chemical reaction: $Si + 2Mg = Mg_2Si$, it was found that one Mg_2Si molecular forms by consuming one Si atom. The densities of Si and Mg_2Si are 2.33 and 1.88 g/cm^3, respectively. Combined with formula: $v = m/\rho$ (volume = mass/density), it was found that 1.24 units volume of Mg_2Si can form by consuming one unit volume of Si. In the Al–20Si–2Mg alloy, no Si atoms were consumed in the formation of primary Mg_2Si, while in the Al–20Si–6Mg alloy most Si atoms were consumed to form primary Mg_2Si. In order, the volume fraction of primary Si and Mg_2Si particles produced from the three alloys was: $V_{Al–20Si–6Mg} > V_{Al–20Si–4Mg} > V_{Al–20Si–2Mg}$.

Compared with the Al–17Si–4Mg alloy, the Al–19Si–4Mg alloy produced more Si atoms, with some primary Mg_2Si particles also formed in the melt. The volume fraction of primary Si and Mg_2Si particles of Al–19Si–4Mg alloy was greater than that of Al–17Si–4Mg alloy. With identical Mg content in the Al–19Si–4Mg, Al–21Si–4Mg, and Al–23Si–4Mg alloys, the volume fraction of primary Mg_2Si particles was the same. In order, the volume fraction of primary Si particles produced in the three alloys was: $V_{Al–23Si–4Mg} > V_{Al–21Si–4Mg} > V_{Al–19Si–4Mg}$. The volume fraction totals of combined primary Si and Mg_2Si particles in the four alloys was: $V_{Al–23Si–4Mg} > V_{Al–21Si–4Mg} > V_{Al–19Si–4Mg} > V_{Al–17Si–4Mg}$.

Determination of particles sizes

As can be seen from Figs. 19 and 21, the variation trend of primary Si particle size distributions of the Al–20Si–2Mg and Al–17Si–4Mg alloys is almost the same: the particle size in the inner layer and out layer is greater than that of the middle layer. Following facts contribute to this size distribution. As melt is poured into the mold, the primary Si particles form rapidly in the outer layer of a casting because of the chilling effect of the mold. Simultaneously, the viscosity of the melt in the out region increases promptly and the primary Mg_2Si particles fail to precipitate at this moment. Hence, in the absence of promotion of Mg_2Si particles, it is difficult for primary Si particles, which form in the outer layer at earlier time, to move toward the inner layer of the tube and they stay and grow up in the outer layer instead. At the same time, primary Si particles which form in the middle layer have some centripetal velocity. According to Eq 2, larger primary Si particles have a greater velocity to move into the inner layer of a tube while smaller Si particles have a less velocity and stay in the middle layer as the viscosity of melt in the middle layer increases.

From Fig. 23, in the inner layer of a tube, the average size of primary Mg_2Si of Al–20Si–6Mg is greater than that of Al–20Si–4Mg as the former alloy has more Mg atoms in the melt. The more Mg atoms will contribute to the nuclei generation and crystal growth of Mg_2Si at the earlier time during solidification. Hence, the primary Mg_2Si particle size is related to the content of Mg.

At the same Si content of 20%, the size of primary Si particles of Al–20Si–6Mg is larger than that of Al–20Si–4Mg. This is related to the volume fraction of the primary Mg_2Si particles in the alloy. The volume fraction of Mg_2Si particles in the Al–20Si–6Mg alloy is greater than that of

Al–20Si–4Mg alloy as shown in Fig. 14. The primary Mg_2Si particles with great volume fraction have greater pushing effect to the primary Si particles under a centrifugal force. Therefore, during the process of the pushing action by primary Mg_2Si particles, plenty of collision, adhesion, and wrapping actions will take place among the primary Si particles [27]. Two or even three primary Si particles will be integrated into one particle. Hence, the size of primary Si particles becomes greater with the increasing content of Mg in the alloy.

It is known that, for the Al–19Si–4Mg, Al–21Si–4Mg, and Al–23Si–4Mg alloys with the same Mg content of 4%, the average size sequence of primary Si particles of the three alloys is: $d_{Al-19Si-4Mg} < d_{Al-21Si-4Mg} < d_{Al-23Si-4Mg}$. This sequence is dependent on the formation sequence of primary Si and Mg_2Si particles. It is known from section "Model establishment of primary particles movement" that the formation of primary Si particles is earlier than that of primary Mg_2Si particles. Therefore, the Si particle size is mainly dependent on the Si content as Mg content is constant in melt. The greater Si content renders it possible for primary Si particles to nucleate and grow up with a greater velocity.

Conclusions

1. When the contents of Si and Mg are equal to or more than 19 and 4%, respectively, the blocky primary Mg_2Si particles, as well as primary Si particles, are formed in the inner cross-sectional layer of the tubes of the hypereutectic aluminum alloy. As a result, the Al–Si–Mg gradient composite tubes were fabricated by centrifugal casting with plentiful blocky primary Si and Mg_2Si particles in the inner layer, no blocky primary Si and Mg_2Si particles in the middle layer, and few blocky primary Si and Mg_2Si particles in the outer layer of the tubes.
2. The morphology of Mg_2Si is the critical characteristic for production of Al–Si–Mg gradient composite tubes. The blocky primary Mg_2Si particles have a relatively greater centripetal velocity, enabling them to move and to push the primary Si particles, which have a relatively smaller centripetal velocity, toward the inner wall of the tubes. The formation of plentiful blocky primary Mg_2Si particles is the key factor to obtain the Al–Si–Mg gradient composites reinforced with primary Si and Mg_2Si particles by centrifugal casting.
3. Calculating the volume fractions of primary Si and Mg_2Si particles in the segregation region of the inner layer in the radial direction, it was found that, with the content of 20% Si unchanged, the mean volume fraction of primary Mg_2Si particles showed an ascending tendency, and that of primary Si particles showed a descending trend as the Mg content gradually increased. With the content of 4% Mg held constant, the average volume fraction of primary Si particles first decreased, and then increased. Average volume fraction of primary Mg_2Si particles rose at first, and then remained in a relatively stable state as the Si content increased gradually.
4. Calculating the sizes of primary Si and Mg_2Si particles in the segregation region of the inner layer of the five alloy tubes, it is concluded that, the average size of primary Si particles is mainly determined by two factors. One is the content of Si. The more the content of Si, the larger the Si particles. The other is the pushing effect of primary Mg_2Si particles to primary Si particles. The greater the volume fraction of primary Mg_2Si particles, the greater the pushing effect and the larger the primary Si particles. The average size of primary Mg_2Si particles is a slight increase as the content of Mg increases.

References

1. Elmadagli M, Perry T, Alpas AT (2007) Wear 262:79
2. Qin QD, Zhao YG, Zhou W (2008) Wear 264:654
3. Edrisy A, Perry T, Alpas AT (2005) Wear 259:1056
4. Edrisy A, Perry T, Cheng YT, Alpas AT (2001) Wear 251:1023
5. Ferrarini CF, Bolfarini C, Kiminami CS, Botta FWJ (2004) Mater Sci Eng A 375–377:577
6. Bobzin K, Ernst F, Richardt K, Schlaefer T, Verpoort C, Flores G (2008) Surf Coat Technol 202:4438
7. Uozato S, Nakata K, Ushio M (2005) Surf Coat Technol 200:2580
8. Tomida S, Nakata K, Shibata S, Zenkouji I, Saji S (2003) Surf Coat Technol 169:468
9. Koizumi M (1997) Composites B 28(1–2):1
10. Kieback B, Neubrand A, Riedel H (2003) Mater Sci Eng A 362:81
11. Fukui Y (1991) JSME Int J III 34:144
12. Duque NB, Melgarejo ZH, Suárez OM (2005) Mater Charact 55(2):167
13. Kang CG, Rohatgi PK (1996) Metals Mater Trans B 27:277
14. Melgarejo ZH, Suarez OM, Sridharan K (2008) Composites A 39(7):1150
15. Matsuda K, Sato R, Watanabe Y (2003) Particle shape distribution in Al-Al3Ni functionally graded materials fabricated by a centrifugal in-situ, method. In: Lo J, Hamada H, Poursartip A, Nakai A, Hoa SV (eds) 4th Joint Canada/Japan Workshop on Composites, Vancouver, Canada, Sep 19–21, 2002, CANMET, Kyoto Inst Technol, Univ British Columbia. Design, Manufacturing and Applications of Composites, pp 77–84
16. Watanabe Y, Oike S (2005) Acta Mater 53(6):1631
17. Watanabe Y, Oike S, Kim IS (2005) Mater Sci Forum 492–493:693
18. Watanabe Y, Nakamura T (2001) Intermetallics 9(1):33
19. Chirita G, Soares D, Silva FS (2008) Mater Des 29(1):20
20. Oya-Seimiya Y, Shinoda T, Fukui Y, Yamaguchi N, Saitou T, Yamada T, Minegishi K (2000) J Jpn Inst Met 64(5):315

21. Oya-Seimiya Y, Shinoda T, Watanabe Y (2002) Adv Fibers Plast Laminates Compos 702:333
22. Zhang J, Fan Z, Wang Y, Zhou B (2000) Mater Des 21(3):149
23. Zhang J, Wang Y, Zhou B, Wu X (1998) J Mater Sci Lett 17:1677
24. Wang Q, Chen Y, Chen W, Wei Y, Zhai C, Ding W (2005) Mater Sci Eng A 394:425
25. Wang Q, Wei Y, Chen W, Zhu Y, Ma C, Ding W (2003) Mater Lett 57:3851
26. Xie Y, Liu C, Zhai Y, Wang K, Ling X (2009) Rare Met 28(4):405
27. Zhai Y, Liu C, Wang K, Zou M, Xie Y (2010) Trans Nonferr Met Soc China 20(3):361
28. Brinkman HC (1952) J Chem Phys 20:571